Geochemistry, Geophysics, Geosystems

RESEARCH ARTICLE
10.1029/2019GC008669

Key Points:
- The outer shell layer of *Tridacna* is depleted in ^{18}O compared to the inner layer, corresponding to a 1.7°C higher reconstructed temperature
- There is no significant difference in $\delta^{13}C$ value between species, but $\delta^{18}O$ is lower in the obligately shallow-dwelling *Tridacna squamosina*
- While carbon isotopes did not track different degrees of photosymbiosis, oxygen isotopes can be used to constrain ecological niche partitioning for rare species

Supporting Information:
- Supporting Information S1
- Data Set S1
- Data Set S2

Correspondence to:
D. Killam,
daniel.e.killam@gmail.com

Citation:
Killam, D., Thomas, R., Al-Najjar, T., & Clapham, M. (2020). Interspecific and intrashell stable isotope variation among the Red Sea giant clams. *Geochemistry, Geophysics, Geosystems*, *21*, e2019GC008669. https://doi.org/10.1029/2019GC008669

Received 3 SEP 2019
Accepted 17 JUN 2020
Accepted article online 22 JUN 2020

Interspecific and Intrashell Stable Isotope Variation Among the Red Sea Giant Clams

Daniel Killam[1,2], Ryan Thomas[1], Tariq Al-Najjar[3], and Matthew Clapham[1]

[1]Department of Earth and Planetary Sciences, University of California, Santa Cruz, CA, USA, [2]Now at Biosphere 2, University of Arizona, Oracle, Arizona, United States, [3]Department of Marine Biology, University of Jordan, Aqaba, Jordan

Abstract The Gulf of Aqaba is home to three giant clam species with differing ecological niches and levels of photosymbiotic activity. Giant clams grow a two-layered shell where the outer layer is precipitated in close association with photosymbiont-bearing siphonal mantle, and the inner layer is grown in association with the light-starved inner mantle. We collected 39 shells of the three species (the cosmopolitan *Tridacna maxima* and *T. squamosa*, as well as the rare endemic *T. squamosina*) and measured carbon and oxygen isotope ratios from inner and outer shell layers, to test for differences among species and between the layers of their shells. *T. squamosina* records higher temperatures of shell formation as determined by oxygen isotope paleothermometry, consistent with its status as an obligately shallow-dwelling species. However, the known negative fractionation imparted on tissue carbon isotopes by photosymbiotic algae did not produce measurable offsets in the carbonate $\delta^{13}C$ values of the more symbiotic *T. squamosina* and *T. maxima* compared to the more heterotrophic *T. squamosa*. Across all species, outer shell layers recorded mean growth temperatures 1.8°C higher than corresponding inner layers, which we propose is a function of the high insolation, low albedo microenvironment of the outer mantle, and potentially the activity of the symbionts themselves. Population-wide isotopic sampling of reef-dwelling bivalve shells can help constrain the ecological niches of rare taxa and help reconstruct their internal physiology.

Plain Language Summary Giant clams are large bivalves which live on reefs and, like corals, also contain algae living as symbionts within their tissue. These clams record temperature via the ratio of two isotopes of oxygen (the heavier ^{18}O and lighter ^{16}O) in their shell, and it has been proposed that their carbon isotope ratios are influenced by their symbionts. The three species of giant clam from around the Gulf of Aqaba (Northern Red Sea): *Tridacna squamosina*, *T. squamosa*, and *T. maxima*, are thought to live in different habitats and to have different amounts of photosynthesis. To test this, we collected several dozen shells to compare the oxygen and carbon isotopes of each species. We found that the rare *T. squamosina* records the highest average growth temperatures, which supports previous observations that it lives only in shallow water. Giant clams also have two layers in their shells, and we compared the isotopes of the layers. We found that the Sun-drenched outer shell layer records higher temperatures than the inner one, which we propose is due to solar heating of the algae-filled outermost tissue. Symbiosis does not appear to change the carbon isotope ratios between the layers or between species with different amounts of photosynthesis. More work is needed to investigate how ecology and physiology influence the isotopes between bivalve species and within their shells.

1. Introduction

The giant clams (Tridacninae) are a subfamily of very large reef-dwelling bivalves with some species growing to over 1.5 m in size (Yonge, 1975). They are also notable for their photosynthetic symbionts, belonging to the same *Symbiodinium* genus found in many reef-building corals, which they cultivate in an altered stomach cavity (Yellowlees et al., 2008). Giant clams are common throughout the lower-latitude Indo-Pacific, but three species are known to inhabit the Red Sea: *Tridacna maxima* Röding, *T. squamosa* Lamarck, and *T. squamosina* Sturany (Richter et al., 2008). *T. maxima* (small giant clam), and *T. squamosa* (fluted giant clam) are globally distributed (Neo et al., 2017), while *T. squamosina* (=*T. costata*, Roa-Quioait et al.) was only recently recognized as a distinct species and is believed to be endemic to the Northern Red Sea (Huber & Eschner, 2010; Richter et al., 2008). The species is extremely rare and potentially endangered today but was the most common *Tridacna* species in Pleistocene fossil reefs (Richter et al., 2008).

Only 13 living specimens of the rare endemic *T. squamosina* were found in prior surveys along the entire Jordanian coast, however, so our understanding of its niche is still limited (Richter et al., 2008). In those underwater surveys, *T. squamosina* was noted to be obligately shallow-dwelling, living epifaunally at the topmost crests of reefs (Richter et al., 2008). In contrast, *T. maxima* inhabits a range of reef depths, and *T. squamosa* is a fore-reef specialist with a solely epifaunal life history (Roa-Quiaoit, 2005). Despite habitat differences, *T. squamosina* and *T. maxima* have similar chlorophyll fluorescence (a measure of photosynthetic activity), implying similarly high levels of reliance on photosymbiotic activity for their food supply (Richter et al., 2008). However, both have stronger chlorophyll fluorescence than the fore-reef *T. squamosa*, which could be more reliant on heterotrophic filter-feeding (Jantzen et al., 2008).

The occurrence of three *Tridacna* species in the Northern Red Sea provides an opportunity to investigate if photosymbiosis alters the carbon isotopic ratios of shell carbonates. Prior studies have attempted to identify a photosymbiotic vital effect influencing the carbonate $\delta^{13}C$ values of giant clams (Jones et al., 1986; Romanek et al., 1987), *Clinocardium nuttalli* (Jones & Jacobs, 1992), and other bivalves (Dreier et al., 2014). The proposed models have taken several forms. Jones et al. (1986) proposed that photosynthesis causes isotopic fractionation that depletes the heavy isotope ^{13}C (a negative shift in $\delta^{13}C$) in shell carbonate compared to gastropods and other neighboring organisms. Other workers proposed that the clam's extrapallial fluid is instead enriched in the heavier ^{13}C isotope because photosymbionts preferentially sequester ^{12}C, leading to higher $\delta^{13}C$ values in shell carbonate during times of greater symbiotic activity (Elliot et al., 2009; McConnaughey et al., 2003). Photosymbiotic corals indeed show such an offset in their shell carbonate (McConnaughey et al., 1997), but it is unclear whether these offsets are consistent across localities and broadly applicable to bivalve taxa such as giant clams, with prior investigations finding inconsistent results (Jones et al., 1988). In the Red Sea, if the McConnaughey model was evident in giant clam carbonate, the $\delta^{13}C$ values of the more symbiotic *T. squamosina* and *T. maxima* would be higher than that of the more heterotrophic *T. squamosa*. Furthermore, *Tridacna* shells contain a prismatic aragonite inner shell layer, precipitated by epithelial cells of the photosynthetically inactive internal mantle. The crossed-lamellar aragonite outer layer is precipitated directly adjacent to the most photosynthetically active siphonal outer mantle (Gannon et al., 2017). Any photosymbiotic effect on the extrapallial fluid of the animal might manifest as a systematic offset between $\delta^{13}C$ values in the inner and outer shell layers. Physiologically driven offsets have been found in heterotrophic bivalves (Trofimova et al., 2018), and we wish to test the hypothesis that differing levels of photosymbiosis will introduce an interspecies spectrum within shell $\delta^{13}C$. An isotopic signal from photosymbiosis could reveal whether ancient reef-building bivalves, such as rudists, lithiotids, and megalodontids, were aided by symbiotic algae, as hypothesized based on their shell morphology (Vermeij, 2013).

Giant clams are well studied as a high-resolution paleotemperature archive, recording conditions at up to daily resolution via the oxygen isotopic ratio of their shell carbonate (Aharon, 1983, 1991; Arias-Ruiz et al., 2017; Duprey et al., 2015; Elliot et al., 2009; Komagoe et al., 2018; Pätzold et al., 1991; Romanek et al., 1987; Watanabe et al., 2004). But these past investigations have all used high-resolution microdrilling sampling to construct time series from a limited number of individuals, in effect measuring a limited number of "trees" at high resolution, with much less focus of the isotopic variability across a "forest" of giant clams. Additionally, aside from the work of Pätzold et al. and Elliot et al., these investigations typically use transects from the inner or outer shell layers of giant clams to reconstruct temperature time series, but not both. However, because an increasing number of studies have identified offsets in paleotemperature estimates constructed from differing shell layers in bivalves (Cusack et al., 2016; Trofimova et al., 2018), a population-wide comparison of inner and outer layers of many individuals would help identify whether such an offset exists for *Tridacna*.

There also is a demand to better understand the comparative ecology of *Tridacna* species in the Northern Red Sea and elsewhere. Giant clams are a broadly distributed subfamily with a high potential for additional cryptic species (Neo et al., 2017) and stable isotope techniques may assist in species recognition if systematic isotopic offsets among species correspond to distinct ecological niches. This method would be especially valuable for rare species such as *T. squamosina* or for morphologically distinctive specimens in historical museum collections. For example, we should be able to corroborate if *T. squamosina* is indeed an obligately shallow reef crest dweller by using shell oxygen isotope ratios to reconstruct growth temperature. The assemblage of Red Sea giant clams provides an opportunity to study the impacts of photosymbiosis on shell carbonate and to constrain the niche partitioning among the species of the region.

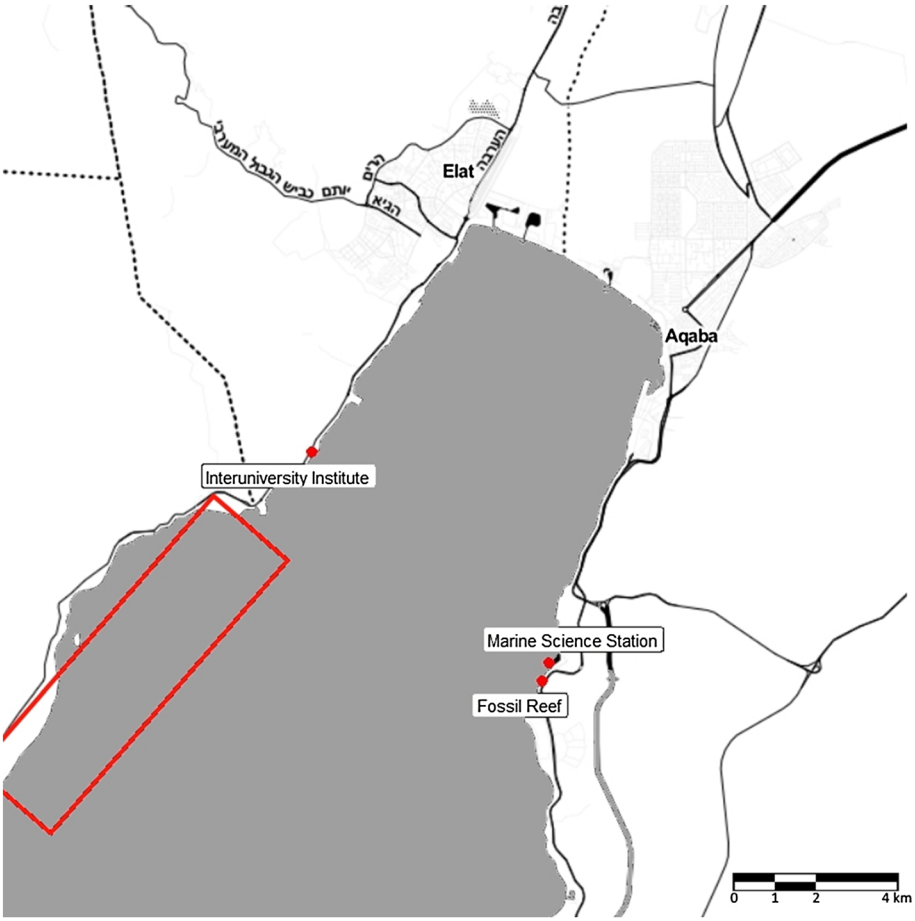

Figure 1. Map of sampling sites used for shells featured in this study, with a red box indicating the potential location of the Sinai shells.

2. Methods

In summer 2016, 39 specimens of *Tridacna* including 5 *T. squamosina*, 15 *T. maxima*, 10 *T. squamosa*, and 9 of undetermined species were collected from beach death assemblages and from shells confiscated at the Egypt border crossing and held at the Hebrew University Museum in Jerusalem (Figure 1 and supporting information). Modern shells (dead individuals collected with permit from the Israeli National Parks Authority) were collected loose in the surf zone, while fossil specimens were sourced from two uplifted reefs. These included one reef previously excavated underneath the Interuniversity Institute in Eilat dated at 2.3 ka (Shaked et al., 2004) and another described as "Terrace R2," south of the Marine Science Station in Aqaba, Jordan, dated as 117 ± 3 ka (Yehudai et al., 2017). Shells were also collected from a reef rock deposit in Eilat called "Tur Yam," dated to 5.6 ka (Weil, 2008), but were not utilized for this study based on poor preservation (supporting information). Species identifications were made according to a key previously used in local studies of *Tridacna* (Roa-Quiaoit, 2005), primarily relying on margin plication morphology, presence of scutes, the size of byssal opening and shell symmetry for identification of the three species in the assemblage. Specimens that were eroded, broken or otherwise unidentifiable are noted as "undetermined," and these shells were used for comparisons of inner and outer shell layer only.

This assemblage represents primarily a juvenile to subadult fauna, with the smallest individual being over a year in age and the largest shell being less than 12 years in age as determined from internal growth couplet counting, which in *Tridacna* has been demonstrated to correspond to true annual periodicity (Pätzold et al., 1991). As such, this study is describing *Tridacna* at an ontogenetic stage when their growth rate is largely constant and not subject to the slowing which happens at maturity in this genus (Klumpp & Griffiths, 1994). The specimens represent a sampling of each subregion in the Gulf of Aqaba (Israel, Jordan and Sinai), which is a small area of ~170 km in length (Figure 1).

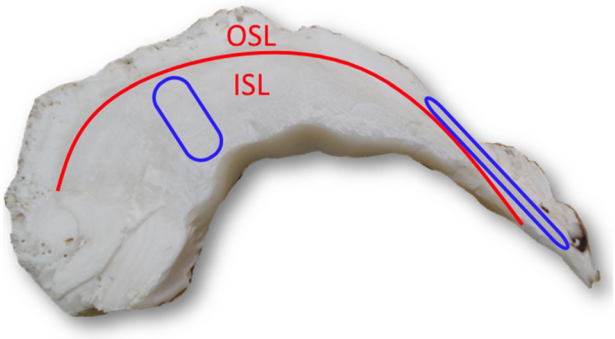

Figure 2. Cross section of a typical specimen of *Tridacna maxima* highlighting the myostracum (boundary between shell layers) in red. Outer shell layer labeled OSL, inner shell layer ISL. Blue ellipses denote the relative sampling location used across all shells.

Shells were sectioned along the axis of maximum growth with a diamond-bladed slow pneumatic saw. The samples were subjected to 1 hr of immersion in a weak 4 weight % sodium hypochlorite solution and then scrubbed with a metal brush to remove encrusting epibionts. Small pieces of each specimen were removed to be surveyed with scanning electron microscopy to confirm original microstructure (Gannon et al., 2017) (supporting information), and then ground and measured with X-ray diffraction spectroscopy to confirm the presence of original aragonite (Kontoyannis & Vagenas, 2000). The cut surfaces were then polished on rotating lathes using successively finer silicon carbide grits down to 18.3 micron size. Samples were then mounted on glass slides and micromilled at 3500 RPM (10% of maximum in order to minimize drill-related fractionation) (Aharon, 1991) with a 0.5-mm Brasseler tungsten carbide drill bit attached to a New Wave micromill to obtain approximately 200 μg of aragonite from the surface of the inner shell layer near the hinge and the outer shell layer near the ventral margin for each sampled shell (Figure 2). Care was taken to average across broad areas of each layer, to ensure averaging across the entire lifespan of the organism. With our youngest individual being more than a year old, this means all shell samples represent at least one complete year of data, and for the larger shells, multiple years. For shells larger than 7-cm length, a handheld Dremel tool with 3-mm tungsten carbide toothed bit set at 200 RPM was used to mill a larger amount (up to 500 μg) of aragonite powder, to ensure that we were measuring a similar relative area of material for small juvenile and more mature specimens.

While sampling in high resolution within both layers of all 39 individuals would have been outside the scope of this study, seven shells were microsampled serially from the outer shell layer to assess the degree to which clams of different species recorded the entire range of seasonal temperatures known from the region. These shells represent multiple species, ontogenetic stages and time periods. Sampling was conducted as a series of short 0.25-cm grooves aligning with microgrowth increments present in the outer shell layer (Gannon et al., 2017).

The samples were homogenized and 50-μg subsamples were then weighed into steel cups and heated overnight at 60°C under vacuum to remove water and volatile organics as part of a lab-standard preventative decontamination procedure. While intercrystalline organics are a trace component of *Tridacna* shell, there is enough to be measured isotopically and potentially introduce contamination that may damage the instrument over time (Dreier et al., 2014). The low roasting temperature was selected to avoid any secondary fractionation of the aragonite which could occur at higher temperatures (Grossman & Ku, 1986). After heating, the samples were placed into glass vials with 1–2 cm of silver wire (to react with sulfur compounds) and acidified at 75°C with water-free orthophosphoric acid in a ThermoScientific Kiel IV Carbonate Device coupled to a ThermoScientific MAT-253 continuous flow Isotope Ratio Mass Spectrometer (IRMS) at UC Santa Cruz. The resulting CO_2 is cryogenically separated in a liquid nitrogen trap and introduced to the IRMS. During an analytical run, samples are standardized relative to Vienna Pee Dee Belemnite (VPDB) versus four NBS-18 limestone standards and an in-house granular Carrara Marble standard (CM12), and two NBS-19 limestone standards are run "as-a-sample" for quality control. Long-term accuracy for 50–70-μg samples is 0.08‰ (VPDB $\delta^{18}O$) and 0.05‰ (VPDB $\delta^{13}C$). All isotope results available in supporting information, along with information on species, locality and other data relevant to the specimen.

$\delta^{18}O$ values were converted to equivalent temperatures of formation using a paleotemperature equation of Grossman and Ku (1986), previously used in other studies of *T. maxima* (Batenburg et al., 2011; Komagoe et al., 2018; Romanek et al., 1987):

$$T\,(^{\circ}\mathrm{C}) = 20.19 - 4.56 * \left(\delta^{18}O - \delta^{18}O_{sw}\right) + 0.19 * \left(\delta^{18}O - \delta^{18}O_{sw}\right)$$

We used a seawater $\delta^{18}O$ value of 1.8‰ relative to Vienna Standard Mean Ocean Water (VSMOW) based on direct measurements from the northern Red Sea (Al-Rousan et al., 2003) and from near the mouth of the Gulf of Aqaba (Andrié & Merlivat, 1989), applying the 0.27‰ correction as discussed in Gonfiantini et al., 1995.

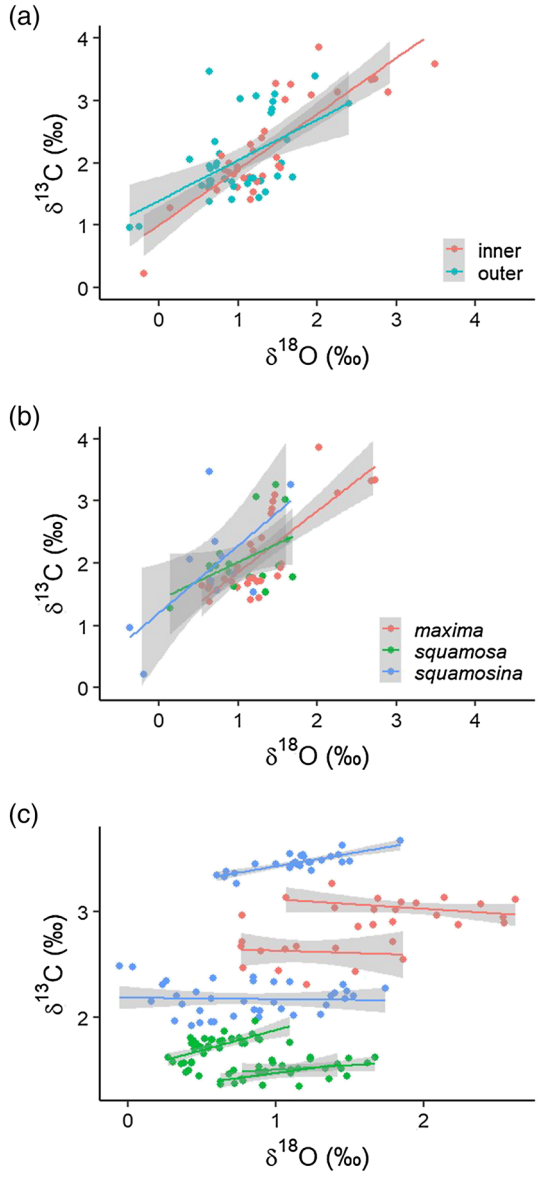

Figure 3. (a) Relationship between $\delta^{18}O$ and $\delta^{13}C$ values by shell layer. (b) Relationship between $\delta^{18}O$ and $\delta^{13}C$ values by species. (c) Relationship between $\delta^{18}O$ and $\delta^{13}C$ values for individual shells (outer layer), collected serially along transects. All equations for plot linear regressions may be found in the supporting information.

Analysis of variance (ANOVA) and Mann-Whitney-Wilcoxon tests were conducted with R software. All statistical tests were assessed for normality and equal variance using Shapiro-Wilk's and Bartlett's tests. Interspecies comparisons displayed normality and equality of variance. When samples from all species were pooled, the sample lacked normality and displayed nonequal variances between inner and outer layers. Comparison of the means between inner and outer layers was subsequently analyzed with the nonparametric Mann-Whitney-Wilcoxon test, and correlations between carbon and oxygen isotope ratios were conducted with Spearman's rank-order correlation. Due to limitations of available specimens, our sample sizes are unbalanced in regard to species and shell layer, with far more specimens of *T. maxima* than the other species, and more examples of outer layers overall for identified specimens due to fragmentation of some shells with loss of the hinge area. As such we have elected for interspecies comparisons to use the outer layer because it is the closest to the exterior environment of the bivalve and the symbiont-rich outer mantle.

3. Data

All isotope results are available in the supporting information, which can also be downloaded from the UC Santa Cruz Dryad open access repository (https://doi.org/10.7291/D13377).

4. Results

Overall, both shell layers exhibit a significant positive correlation between $\delta^{13}C$ and $\delta^{18}O$ values. Although the correlation is stronger for the inner layer (inner: rho = 0.727, $p < 0.00005$; outer: rho = 0.375, $p < 0.05$) (Figure 3), a nonparametric analysis of covariance shows that the relationships for the inner and outer layer are not significantly different ($h = 0.315$, p value = 0.3759) (Young & Bowman, 1995). The outer shell layers across all specimens record a higher reconstructed temperature (22.7°C) than the inner layer (21.0°C) (Table 1; paired Wilcoxon signed rank test, $V = 923.5$, p value = 0.019). In contrast, we did not detect a difference in $\delta^{13}C$ values between the inner and outer layers ($V = 564$, $p = 0.145$).

The relationship between $\delta^{13}C$ and $\delta^{18}O$ is positive for bulk data for all three species, across both shell layers (Figures 3a and 3b). However, this correlation is not universal when observing the correlation within individuals (Figure 3c). Comparing outer shell layer values between species, *T. squamosina* has a 3°C higher reconstructed temperature than the others, while the other species display similar mean values to each other (Table 1). With a one-way ANOVA, we confirmed a difference at the $\alpha = 0.005$ level among the three species ($F(2,28) = 6.46$, $p = 0.0049$). A post hoc Tukey test shows that while *T. squamosina* is different from the other two species, we did not detect a difference between *T. squamosa* and *T. maxima*. (Table 2). A one-way ANOVA does not confirm a significant variation in $\delta^{13}C$ values between the outer layers of each species ($F(2,28) = 0.103$, $p = 0.902$; Figure 4b).

Comparing the isotopic transects of the seven individuals, all record temperatures in a restricted seasonal range typical of the Red Sea, with ~5–9°C separating the summer highs and winter lows (Figure 5). J44, a modern example of *T. maxima* from Jordan, shows lower temperatures at the end of its recorded transect, while H5, an example of *T. squamosina* from Sinai, shows high summer temperatures above 29°C. Not all specimens have a complete annual oscillation present as measured by peak-to-peak growth, but all appear to have growth above 2 cm/year, and H5 is faster, growing over 6 cm/year for one of its annual oscillations. Carbon isotopes do not show the same seasonality within individuals, with most of the shells displaying comparatively static values (Figure 5).

Table 1
Means of Isotope Ratios, Standard Deviations (SD), and Calculated Temperatures of Shell Layers

		$\delta^{13}C$ (‰)		$\delta^{18}O$ (‰)		Temperature (°C)	
Shell layer	*N*	Mean	SD	Mean	SD	Mean	SD
Outer, all specimens	39	1.9	1.0	1.0	0.6	22.7	2.7
Inner, all specimens	36	2.2	0.8	1.4	0.7	21.0	3.2
Outer, *T. squamosina*	5	2.1	0.9	0.4	0.5	25.1	1.9
Inner, *T. squamosina*	6	1.8	1.0	0.9	0.6	23.1	2.7
Outer, *T. squamosa*	9	2.0	0.5	1.1	0.4	22.2	1.8
Inner, *T. squamosa*	8	2.1	0.7	1.1	0.5	23.2	2.1
Outer, *T. maxima*	17	2.0	0.6	1.1	0.4	22.0	1.5
Inner, *T. maxima*	15	2.3	0.8	1.4	0.7	20.6	2.9

5. Discussion

5.1. No Shell Carbon Isotope Link With Photosymbiosis

We did not find a ^{13}C enrichment in either the outer or inner shell layers of the three *Tridacna* species, despite our previous expectation that *T. squamosina* and *T. maxima* would display higher values in the outer layer based on their greater photosymbiotic activity (Jantzen et al., 2008). Prior investigations of *T. gigas* from other regions found higher $\delta^{13}C$ values in the outer layer (Elliot et al., 2009; Gannon et al., 2017), possibly because photosymbionts in the siphonal mantle adjacent to the outer shell layer drew down the lighter ^{12}C available in the calcifying fluid. The lack of difference in $\delta^{13}C$ values between inner and outer shell layers of *T. squamosina, T. maxima*, and *T. squamosa* could occur because these three species are smaller than mature specimens of *T. gigas*, as previous studies have found size-dependent increases in photosynthetic productivity among giant clams (Yau & Fan, 2012). The smaller size of the studied species may also lead to less spatial isolation between their symbiont-rich siphonal mantle and the symbiont-barren inner mantle, leading to a lack of differential ^{12}C drawdown between the shell layers.

The relationship between carbon and oxygen isotope ratios is significant and consistent across layers and between species, though the slope is small (Figures 3a and 3b). Such positive correlations have been noted by some workers as a sign of a kinetic isotope effect in coral skeletons, originating from the incomplete equilibration with calcification site dissolved inorganic carbonate (DIC), but kinetic effects are less likely to occur in mollusks due to their use of ambient DIC for calcification (McConnaughey & Gillikin, 2008). Positive correlations have been observed in other giant clam species (Romanek et al., 1987; Watanabe et al., 2004), although not universally (Aharon, 1991), and have been proposed to be caused by seasonal control of photosymbiosis (Elliot et al., 2009; McConnaughey & Gillikin, 2008; Romanek et al., 1987). However, the $\delta^{13}C$ records lack seasonality in the studied Red Sea clams measured via high-resolution transects (Figure 5), making this explanation less likely for the Aqaba giant clams. This lack of seasonality in $\delta^{13}C$ has been observed in other *Tridacna* stable isotope studies (Elliot et al., 2009; Yamanashi et al., 2016).

In the case of our data, the correlation between $\delta^{13}C$ and $\delta^{18}O$ is noted for both inner and outer shell layers across multiple individuals and is not significantly weaker in the inner layer, which is isolated from the activity of symbionts. We suggest that the correlation may be related to environmental factors influencing the $\delta^{13}C$ values of ambient DIC or the phytoplankton-sourced carbon that is respired and subsequently integrated into giant clam carbonate. The positive correlation is unlikely to reflect photosymbiosis in the Red Sea clams, as corals of the region show a negative correlation between $\delta^{13}C$ and $\delta^{18}O$, attributed to low winter insolation limiting symbiont activity (Erez, 1978; Klein et al., 1992), not positive as observed in corals from other regions (McConnaughey et al., 1997; Swart et al., 1996). The variety of carbon sources (environmental DIC, respired CO_2 from both endogenous and exogenous food) and the conflicting variations in these sources make tridacnid shell carbonate an integration of numerous interacting effects, as in corals. For example, mean $\delta^{13}C$ of a coral skeleton was found to decline in $\delta^{13}C$ and increase in mean $\delta^{18}O$ when the colony was transplanted from 6 to 40 m in the Gulf of Aqaba, which was proposed to be a mixture of differential kinetic and symbiotic effects between deep and shallow-water life habits (Rosenfeld et al., 2003). The lack of large intrashell $\delta^{13}C$ variability of our transected shell records, but larger intershell variability for both the transect means and bulk-sampled data (Figures 3c and 5), suggests that differing conditions across the reef are the main control on Red Sea giant clam $\delta^{13}C$. Such trends could explain the broader correlation across our sampled population and its lack within some individuals (Figure 3c). Long-term observation of giant clams sourced from different reef microenvironments, combined with detailed isotopic measurement and modeling of the interaction of carbon reservoirs inside and outside the organism will be needed to settle the specific cause of the positive isotope correlation often observed in giant clams.

Although shell $\delta^{13}C$ values did not differ significantly among the three species, *T. squamosina* has a slightly higher $\delta^{13}C$ and

Table 2
Tukey HSD Results for the Analysis of Variance for Temperature Differences Between the Species

Species comparison	Difference	Lower	Upper	*p* value (adjusted)
squamosa-maxima	0.179	−1.57	1.93	0.965
squamosina-maxima	3.06	0.905	5.22	0.004
squamosina-squamosa	2.88	0.518	5.25	0.014

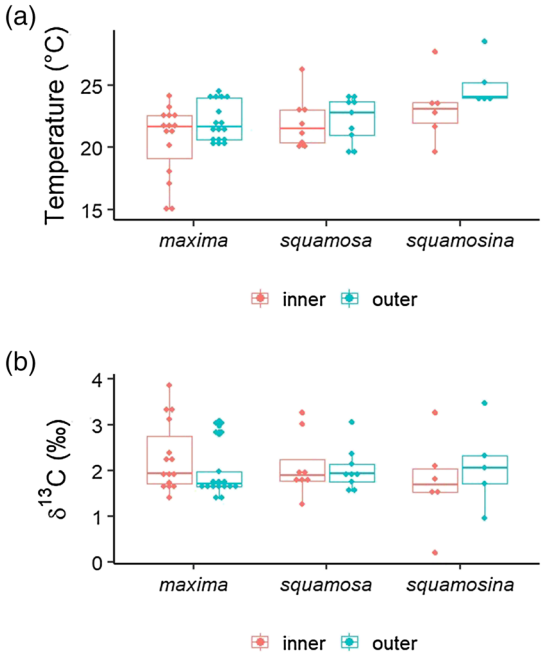

Figure 4. (a) Distributions of δ^{18}O-derived temperatures for the three species, inner and outer shell layers. Horizontal lines are the medians, middle quartiles contained in boxes, whiskers are 1.5 times the interquartile range, and solid points are outliers. (b) Distributions of δ^{13}C values for the three species and their respective shell layers.

T. maxima has the lowest mean value (Table 1 and Figure 4b). These trends do not align with an expectation that the two more photosymbiotic species (*T. squamosina* and *T. maxima)* would have higher δ^{13}C values than *T. squamosa*. Because giant clams have a large volume of extrapallial fluid that is continuously exchanged with seawater (Ip et al., 2017), symbiont photosynthetic fractionation could be too small to overprint environmental influences and enrich shell carbonate δ^{13}C. The δ^{13}C values of *Tridacna* tissues also display little of the negative offset expected from a diet rich in photosynthate, because their symbionts are carbon-limited and produce sugars with reduced fractionation (Johnston et al., 1995). This reduced degree of fractionation combined with a large reservoir of environmentally sourced extrapallial fluid may overwhelm any photosymbiotic offset that would be expected to appear in giant clam carbonate, even in our favorable test system of three species within the same environment. The large range of δ^{13}C values across these populations of closely associated tridacnids further suggests that microenvironmental influences may play a significant role in their shell carbon isotope composition.

5.2. Shell δ^{18}O-Derived Temperatures as a Marker of Tridacna Species-Specific Niche

Oxygen isotope ratios of *T. squamosina* imply temperatures 3°C warmer (95% CI: 0.9–5.2°C) than *T. maxima* and a similar offset compared to *T. squamosa*, though a Tukey post hoc test demonstrated there was no significant difference for the two more common species compared to each other (Table 2 and Figure 4a). This is not an insignificant difference for reef environments, as the Northern Red Sea experiences a relatively restricted annual temperature range between 21°C and 28°C (Edwards, 1987). These results corroborate previous underwater transect observations that *T. squamosina* is an obligate shallow-water dweller present only on the reef crest and reef flat (Richter et al., 2008; Roa-Quiaoit, 2005). *T. maxima* in the region has been proposed to inhabit a broader range of depths, whereas *T. squamosa* has been interpreted as a fore-reef specialist due to its greater reliance on heterotrophy (Jantzen et al., 2008; Roa-Quiaoit, 2005).

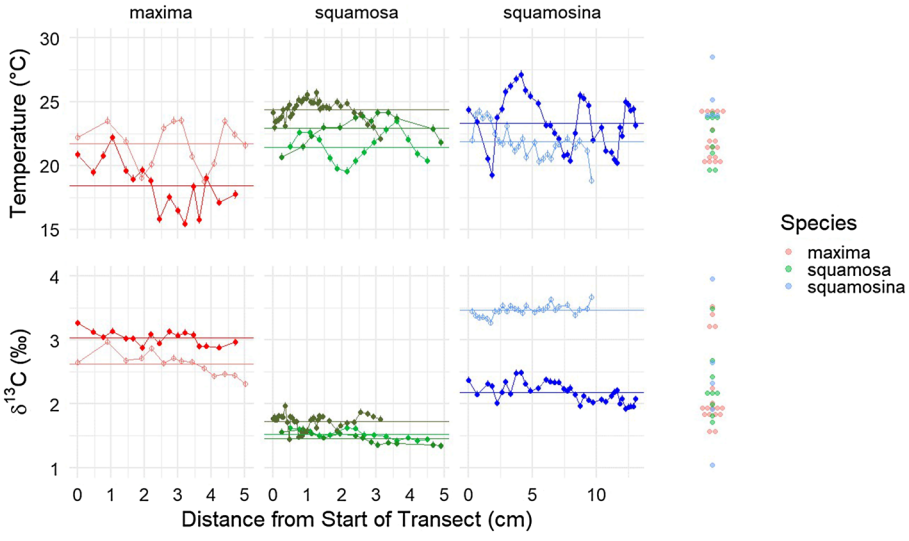

Figure 5. Isotopic transects through seven specimens of three species, showing the time series of temperatures recorded via microsampled oxygen isotope paleothermometry of outer shell layers. Transects begin at differing ontogenetic points between individuals. The dot plot to the right shows distributions of temperatures recorded by bulk sampled outer shell layers. Color corresponds to species. Lighter-colored time series with open circles are Last Interglacial in age. Colored horizontal lines indicate means of individual time series.

Past studies of *T. maxima*, *T. gigas*, *T. squamosa*, and other giant clams have used paleotemperature equations that are close variations of the equation developed by Grossman and Ku (1986) (Batenburg et al., 2011; Komagoe et al., 2018; Romanek et al., 1987; Watanabe et al., 2004). As *T. squamosina* is closely related to *T. maxima* (Richter et al., 2008), a species which has been previously been demonstrated to precipitate aragonite in oxygen isotope equilibrium with seawater, like all other tested *Tridacna* species (Romanek et al., 1987), species-specific differences in calcification mechanisms likely cannot explain the warmer temperatures recorded in *T. squamosina* shells. All three species record temperatures in the range of that expected of the Northern Red Sea (Edwards, 1987) (Figure 5).

Our data include fossil and modern specimens, but while *T. maxima* is predominant among our fossil collection, we do not believe recent ocean warming explains the species-specific differences present in our work. Previous work has demonstrated that mean annual sea surface temperatures were almost the same (within 0.5°C) in the late Holocene (Felis et al., 2004) and "indistinguishable from the 1995 to 2014 mean" at the last interglacial (Hoffman et al., 2017), though seasonality is thought to have been higher. To this effect, the two shells microsampled from the Last Interglacial-aged terrace in Jordan record temperatures within the same range as the modern shells (Figure 5). Because of this, comparison of bulk oxygen isotopes between fossil and modern individuals in the Northern Red Sea is likely to be a function more of site and microenvironment rather than climatic differences.

The Red Sea displays little temperature gradient with depth compared to other water bodies, but reefs of the Northern Red Sea can display enough temperature variability to explain the disparity between the *Tridacna* species in our data set. Fringing reefs of the region display higher temperature than the reef slope due to trapped, thermally stratified water, with about a 1.2°C difference in mean temperature experienced between corals at 7- versus 42-m water depth in Jordanian coastal waters (Al-Rousan et al., 2003). Spatiotemporal variability is quite high on diurnal scales (Monismith et al., 2006), but in general, average temperature should decrease with depth, particularly at microenvironmental scale on the reef. In addition, researchers have determined that corals increase the temperature of their local microenvironment by up to 1.5°C on top of existing temperature variability due to the combined influences of their own albedo and disturbance of laminar flow (and therefore less heat exchange with cooler water) (Fabricius, 2006; Jimenez et al., 2011). The shallowest portion of the reef may reach even warmer temperatures than ambient sea surface temperature if they experience tidal emersion and exposure to warmer air temperatures (Head, 1987; Schoepf et al., 2015), and on the shallow reef, the heating impact of insolation can be dramatic, with up to 2.2°C differences in temperature between shaded and unshaded areas (Bahr et al., 2018).

Oxygen isotope ratios in the three Red Sea species are lower in the outer shell layer, suggesting a temperature elevated by ~1.7°C relative to the inner layer. This aligns with a previous study which found outer shell layer paleotemperatures 0.6°C higher than those of the inner layer, though comparing the two layers was not the aim of their experiment (Pätzold et al., 1991). A different study of *T. gigas* from another locality found an opposite relationship, with the inner layer recording slightly higher temperatures (Elliot et al., 2009). In other bivalve taxa, different biomineralization processes between the outer crossed-lamellar and inner prismatic shell layers may cause different isotopic fractionation. Trofimova et al. (2018) found lower $\delta^{18}O$ values in the outermost homogenous prismatic/granular portion of the outer shell layer of *Arctica islandica* relative to the crossed-acicular/lamellar inner portion of the outer layer. This opposes the pattern in *Tridacna*, which have lower $\delta^{18}O$ values in their crossed-lamellar shell layer. The inner prismatic layer recorded higher $\delta^{18}O$ values in *Modiolus modiolus* (Cusack et al., 2016), which appears more analogous to what we observe in *Tridacna*, but the outer shell layer in *Modiolus* was nacreous, rather than crossed lamellar.

Although fractionation on the basis of microstructure cannot be ruled out, the conflicting outer layer offsets in the previous studies of *Tridacna* (Elliot et al., 2009; Pätzold et al., 1991) suggest that $\delta^{18}O$ differences may reflect actual temperature variations rather than conserved, universal effects resulting from the differences between microstructure types in *Tridacna* shells. The outer mantle is a lower albedo tissue exposed to greater solar radiation and heat produced by the dissipation of light energy within the photosystems of the *Symbiodinium* chloroplasts (Yau & Fan, 2012). In contrast, the inner mantle is largely shaded from sunlight and has fewer symbiont tubules than the siphonal mantle (Ip et al., 2017, 2018; Norton & Jones, 1992). This difference in mantle microenvironments could explain the difference in calculated temperature between the inner and outer mantles of the giant clams, analogous to the differences in $\delta^{18}O$ values between corallites on

the Sun-drenched "bumps" and shaded "valleys" of coral heads (Cohen & Hart, 1997). The shallowest and most sunlight-exposed *T. squamosina* displays a larger inner-outer difference than the other species (Figure 4a), as would be expected for the shallowest species experienceing the strongest insolation-related warming. In contrast, *Tridacna* specimens located deeper on the reef or in shaded areas may not display this effect.

Additionally, our bulk sampling approach requires consideration of the prospect that the growth layers are vulnerable to differential time averaging. Could the outer growth layer record higher mean temperature due to a cessation of growth in winter months, while the inner layer continues to grow during that colder time? As a tropical bivalve, *Tridacna* is generally known for year-round growth (Killam & Clapham, 2018), but slowdowns of growth must be considered even if they lack a complete cessation. One of the serially sampled shells records temperatures well under 20°C (Figure 5). Therefore, the higher mean temperatures seen in the outer layer of our shells are unlikely be a function of the outer layer ceasing growth in winter. Meanwhile from the opposing perspective, the cooler temperature of the inner layer could also be caused by a lack of summer growth in that layer preferentially. Prior studies using the inner layer of *T. gigas* found in Palau determined it was able to measure the entire seasonal amplitude of temperatures between 22°C and 28°C (Pätzold et al., 1991) and similarly up to 28.5°C for *T. squamosa* (Arias-Ruiz et al., 2017), which is around the same maximum known from the Northern Red Sea. Therefore, we also assume that the lower temperature estimate from the interior layer of our shells is not the result of a summer high temperature cessation preferentially influencing the inner layer.

While our chosen sampling location for the outer shell layer is recorded later in the animal's ontogeny, even the oldest clam used in this data set is younger than the age at which senescence begins to lead to slower growth in *Tridacna maxima*, around 15 years (Romanek et al., 1987). As giant clams slow their growth even approaching 60 years in age, they continue to record the same amplitude of oxygen isotope-based paleotemperatures if sampled at sufficient resolution (Watanabe et al., 2004; Welsh et al., 2011). Over the course of four seasonal oscillations recorded within shell H5, a modern specimen of *T. squamosina* from Sinai, no modulation of recorded temperatures could be observed across the record, even at a relatively coarse sampling resolution (Figure 5). In the case of bulk sampling, the issue of resolution is negated by seasonal oscillations being homogenized into one sample. The limited number of serial-sampled means and bulk sampled values plot within similar ranges by species (Figure 5).

5.3. Significance of Comparative Ecology via Shell Isotope Analysis for Closely Related Species

In our investigation of the isotope ratios recorded in the shells of Red Sea giant clams, we have found variability within and between shells with relevance for further work investigating the ecology and geochemistry of tridacnids and other bivalves. The lower oxygen isotope ratios recorded in the outer shell layer versus the inner layer suggests attention should be paid to the shell regions used when comparing the results of separate reconstructions. Additional investigations of intrashell oxygen isotope variability will be needed for other bivalve taxa, which are paleoclimate proxy targets (Cusack et al., 2016; Trofimova et al., 2018). We also found that shell carbon isotope ratios did not conform with known variations in photosymbiotic activity between closely related giant clam species, suggesting that different proxies should be prioritized in future efforts to identify photosymbiosis in fossil bivalves.

Of the three *Tridacna* species found in the region, *T. squamosina* is the rarest and believed to be endemic to the Northern Red Sea (Neo et al., 2017). In their initial description of the species, Richter et al. (2008) noted that it represents less than 5% of the life assemblage ($n = 13$) as observed during underwater transects. Using shell remains, we have found oxygen isotope ratios corroborating the previous work describing *T. squamosina* as an obligate shallow reef-dwelling species.

Fossil reefs are important archives of baseline reef community structure, which in some cases can be more accurate in assessing the true diversity of the reef biome than both life and death assemblages alone (Edinger et al., 2001). When endangered endemics such as *T. squamosina* are at risk of disappearing before they are fully described (Lees & Pimm, 2015), the comparative isotopic analysis of reef fossils will become more important in characterizing the full preindustrial niches of vulnerable species too rare to observe in large sample sizes in the wild, particularly in regions such as the Red Sea which were not described by SCUBA transect observations until relatively recently. Stable isotope approaches have already proven useful for

description of cryptic marine vertebrates (Owen et al., 2011). As new cryptic species of *Tridacna* and other vulnerable reef organisms continue to be genetically described (Fauvelot et al., 2020; Huelsken et al., 2013; Monsecour, 2016; Su et al., 2014), stable isotope techniques may prove increasingly necessary to characterize their comparative ecology.

Data Availability Statement

All data used in this study are available in as "Supplemental Data" in the supporting information and also have been submitted to the UC Santa Cruz Dryad repository (available here: https://doi.org/10.7291/D13377).

Conflict of Interest

On behalf of all authors, the corresponding author states that there is no conflict of interest.

Acknowledgments

We wish to thank Colin Carney and Dyke Andreasen at the UCSC Stable Isotope Laboratory and Tom Yuzhvinsky at the UCSC W.M. Keck Center for Nanoscale Optofluidics. Brandon Cheney (UCSC Earth and Marine Sciences) assisted with collection and interpretation of XRD results. Moty Ohevia, Adina Paytan, Michele Markowitz, Karen Petersen, and Noam Baharav assisted with fieldwork. Henk Mienis (Hebrew University Museum), Muki Shpigel (National Center for Mariculture, Eilat) and Yonathan Shaked provided access to specimens and advice on localities. Asaph Zvuloni (Israel Nature and Parks Authority) provided permit assistance and supervised collection along the protected coastline of Eilat. Paul Koch, James Zachos and Kristy Kroeker (UC Santa Cruz) provided comments and suggestions for the manuscript, as well as Dr. Paul Aharon (University of Alabama) and other anonymous reviewers. Funding for research and travel was provided by the UCSC Casey Moore Fund, AMNH Lerner-Grey Foundation, Myers Oceanographic Trust, and NSF Coastal IRES program. The Interuniversity Institute in Eilat provided access to work resources and their protected reef.

References

Aharon, P. (1983). 140,000-yr isotope climatic record from raised coral reefs in New Guinea. *Nature*, *304*(5928), 720–723. https://doi.org/10.1038/304720a0

Aharon, P. (1991). Recorders of reef environment histories: Stable isotopes in corals, giant clams, and calcareous algae. *Coral Reefs*, *10*(2), 71–90. https://doi.org/10.1007/BF00571826

Al-Rousan, S., Al-Moghrabi, S., Pätzold, J., & Wefer, G. (2003). Stable oxygen isotopes in *Porites* corals monitor weekly temperature variations in the northern Gulf of Aqaba, Red Sea. *Coral Reefs*, *22*(4), 346–356. https://doi.org/10.1007/s00338-003-0321-6

Andrié, C., & Merlivat, L. (1989). Contribution des données isotopiques de deutérium, oxygène-18, hélium-3 et tritium, à l'étude de la circulation de la Mer Rouge. *Oceanologica Acta*, *12*(3), 165–174. https://doi.org/10.1016/s0399-1784(00)01121-x

Arias-Ruiz, C., Elliot, M., Bézos, A., Pedoja, K., Husson, L., Cahyarini, S. Y., et al. (2017). Geochemical fingerprints of climate variation and the extreme La Niña 2010–11 as recorded in a *Tridacna squamosa* shell from Sulawesi, Indonesia. *Palaeogeography, Palaeoclimatology, Palaeoecology*, *487*, 216–228. https://doi.org/10.1016/j.palaeo.2017.08.037

Bahr, K. D., Jokiel, P. L., & Rodgers, K. S. (2018). Influence of solar irradiance on underwater temperature recorded by temperature loggers on coral reefs. *Limnology and Oceanography: Methods*, *14*(5), 338–342. https://doi.org/10.1002/lom3.10093

Batenburg, S. J., Reichart, G.-J., Jilbert, T., Janse, M., Wesselingh, F. P., & Renema, W. (2011). Interannual climate variability in the Miocene: High resolution trace element and stable isotope ratios in giant clams. *Palaeogeography, Palaeoclimatology, Palaeoecology*, *306*(1-2), 75–81. https://doi.org/10.1016/j.palaeo.2011.03.031

Cohen, A. L., & Hart, S. R. (1997). The effect of colony topography on climate signals in coral skeleton. *Geochimica et Cosmochimica Acta*, *61*(18), 3905–3912. https://doi.org/10.1016/S0016-7037(97)00200-7

Cusack, M., Parkinson, D., Freer, A., Pérez-Huerta, A., Fallick, A. E., & Curry, G. B. (2016). Oxygen isotope composition in Modiolus modiolus aragonite in the context of biological and crystallographic control. *Mineralogical Magazine*, *72*(2), 569–577. https://doi.org/10.1180/minmag.2008.072.2.569

Dreier, A., Loh, W., Blumenberg, M., Thiel, V., Hause-Reitner, D., & Hoppert, M. (2014). The isotopic biosignatures of photo-vs. thiotrophic bivalves: Are they preserved in fossil shells? *Geobiology*, *12*(5), 406–423. https://doi.org/10.1111/gbi.12093

Duprey, N., Lazareth, C. E., Dupouy, C., Butscher, J., Farman, R., Maes, C., & Cabioch, G. (2015). Calibration of seawater temperature and $\delta^{18}O_{seawater}$ signals in *Tridacna maxima*'s $\delta^{18}O_{shell}$ record based on in situ data. *Coral Reefs*, *34*(2), 437–450. https://doi.org/10.1007/s00338-014-1245-z

Edinger, E. N., Pandolfi, J. M., & Kelley, R. A. (2001). Community structure of Quaternary coral reefs compared with Recent life and death assemblages. *Paleobiology*, *27*(4), 669–694. https://doi.org/10.1666/0094-8373(2001)027%3C0669:CSOQCR%3E2.0.CO;2

Edwards, F. J. (1987). Climate and oceanography. F. J. Edwards & S. M. Head. In *Red Sea* (Vol. 1, pp. 45–68). Oxford, UK: Pergamon.

Elliot, M., Welsh, K., Chilcott, C., McCulloch, M., Chappell, J., & Ayling, B. (2009). Profiles of trace elements and stable isotopes derived from giant long-lived *Tridacna gigas* bivalves: Potential applications in paleoclimate studies. *Palaeogeography, Palaeoclimatology, Palaeoecology*, *280*(1-2), 132–142. https://doi.org/10.1016/j.palaeo.2009.06.007

Erez, J. (1978). Vital effect on stable-isotope composition seen in foraminifera and coral skeletons. *Nature*, *273*(5659), 199–202. https://doi.org/10.1038/273199a0

Fabricius, K. E. (2006). Effects of irradiance, flow, and colony pigmentation on the temperature microenvironment around corals: Implications for coral bleaching? *Limnology and Oceanography*, *51*(1), 30–37. https://doi.org/10.4319/lo.2006.51.1.0030

Fauvelot, C., Zuccon, D., Borsa, P., Grulois, D., Magalon, H., Riquet, F., et al. (2020). Phylogeographical patterns and a cryptic species provide new insights into Western Indian Ocean giant clams phylogenetic relationships and colonization history. *Journal of Biogeography*, *47*(5), 1086–1105. https://doi.org/10.1111/jbi.13797

Felis, T., Lohmann, G., Kuhnert, H., Lorenz, S. J., Scholz, D., Pätzold, J., et al. (2004). Increased seasonality in Middle East temperatures during the last interglacial period. *Nature*, *429*(6988), 164–168. https://doi.org/10.1038/nature02546

Gannon, M. E., Pérez-Huerta, A., Aharon, P., & Street, S. C. (2017). A biomineralization study of the indo-Pacific giant clam *Tridacna gigas*. *Coral Reefs*, *36*(2), 503–517. https://doi.org/10.1007/s00338-016-1538-5

Gonfiantini, R., Stichler, W., & Rozanski, K. (1995). *Standards and intercomparison materials distributed by the International Atomic Energy Agency for stable isotope measurements*, Vienna, Austria: . IAEA-TECDOC—825. IAEA.

Grossman, E. L., & Ku, T.-L. (1986). Oxygen and carbon isotope fractionation in biogenic aragonite: Temperature effects. *Chemical Geology: Isotope Geoscience Section*, *59*, 59–74. https://doi.org/10.1016/0168-9622(86)90057-6

Head, S. M. (1987). Corals and coral reefs of the Red Sea. In *Red Sea* (pp. 128–151). Oxford, UK: Pergamon Press.

Hoffman, J. S., Clark, P. U., Parnell, A. C., & He, F. (2017). Regional and global sea-surface temperatures during the last interglaciation. *Science*, *355*(6322), 276–279. https://doi.org/10.1126/science.aai8464

Huber, M., & Eschner, A. (2010). *Tridacna (Chametrachea) costata* Roa-Quiaoit, Kochzius, Jantzen, Al-Zibdah & Richter from the Red Sea, a junior synonym of *Tridacna squamosina* Sturany, 1899 (Bivalvia, Tridacnidae). *Annalen des Naturhistorischen museums in Wien. Serie B Für Botanik und Zoologie*, 153–162.

Huelsken, T., Keyse, J., Liggins, L., Penny, S., Treml, E. A., & Riginos, C. (2013). A novel widespread cryptic species and phylogeographic patterns within several giant clam species (Cardiidae: Tridacna) from the Indo-Pacific Ocean. *PLoS ONE*, *8*(11), e80858. https://doi.org/10.1371/journal.pone.0080858

Ip, Y. K., Hiong, K. C., Goh, E. J. K., Boo, M. V., Choo, C. Y. L., Ching, B., et al. (2017). The whitish inner mantle of the giant clam, *Tridacna squamosa*, expresses an apical plasma membrane Ca^{2+}-ATPase (PMCA) which displays light-dependent gene and protein expressions. *Frontiers in Physiology*, *8*. https://doi.org/10.3389/fphys.2017.00781

Ip, Y. K., Koh, C. Z. Y., Hiong, K. C., Choo, C. Y. L., Boo, M. V., Wong, W. P., et al. (2018). Carbonic anhydrase 2-like in the giant clam, *Tridacna squamosa*: Characterization, localization, response to light, and possible role in the transport of inorganic carbon from the host to its symbionts. *Physiological Reports*, *5*(23), e13494. https://doi.org/10.14814/phy2.13494

Jantzen, C., Wild, C., El-Zibdah, M., Roa-Quiaoit, H. A., Haacke, C., & Richter, C. (2008). Photosynthetic performance of giant clams, *Tridacna maxima* and *T. squamosa*, Red Sea. *Marine Biology*, *155*(2), 211–221. https://doi.org/10.1007/s00227-008-1019-7

Jimenez, I. M., Kühl, M., Larkum, A. W. D., & Ralph, P. J. (2011). Effects of flow and colony morphology on the thermal boundary layer of corals. *Journal of the Royal Society Interface*, *8*(65), 1785–1795. https://doi.org/10.1098/rsif.2011.0144

Johnston, M., Yellowlees, D., & Gilmour, I. (1995). Carbon isotopic analysis of the free fatty acids in a tridacnid-algal symbiosis: Interpretation and implications for the symbiotic association. *Proceedings of the Royal Society of London B*, *260*(1359), 293–297. https://doi.org/10.1098/rspb.1995.0094

Jones, D. S., & Jacobs, D. K. (1992). Photosymbiosis in *Clinocardium nuttalli*: Implications for tests of photosymbiosis in fossil molluscs. *PALAIOS*, *7*(1), 86–95. https://doi.org/10.2307/3514798

Jones, D. S., Williams, D. F., & Romanek, C. S. (1986). Life history of symbiont-bearing giant clams from stable isotope profiles. *Science*, *231*(4733), 46–48. https://doi.org/10.1126/science.231.4733.46

Jones, D. S., Williams, D. F., & Spero, H. J. (1988). More light on photosymbiosis in fossil mollusks: The case of *Mercenaria* "tridacnoides.". *Palaeogeography, Palaeoclimatology, Palaeoecology*, *64*(3-4), 141–152. https://doi.org/10.1016/0031-0182(88)90003-X

Killam, D. E., & Clapham, M. E. (2018). Identifying the ticks of bivalve shell clocks: Seasonal growth in relation to temperature and food supply. *PALAIOS*, *33*(5), 228–236. https://doi.org/10.2110/palo.2017.072

Klein, R., Pätzold, J., Wefer, G., & Loya, Y. (1992). Seasonal variations in the stable isotopic composition and the skeletal density pattern of the coral *Porites lobata* (Gulf of Eilat, Red Sea). *Marine Biology*, *112*(2), 259–263. https://doi.org/10.1007/BF00702470

Klumpp, D. W., & Griffiths, C. L. (1994). Contributions of phototrophic and heterotrophic nutrition to the metabolic and growth requirements of four species of giant clam (Tridacnidae). *Marine Ecology Progress Series*, *115*, 103–115. https://doi.org/10.3354/meps115103

Komagoe, T., Watanabe, T., Shirai, K., Yamazaki, A., & Uematu, M. (2018). Geochemical and microstructural signals in giant clam *Tridacna maxima* recorded typhoon events at Okinotori Island, Japan. *Journal of Geophysical Research: Biogeosciences*, *123*, 1460–1474. https://doi.org/10.1029/2017JG004082

Kontoyannis, C. G., & Vagenas, N. V. (2000). Calcium carbonate phase analysis using XRD and FT-Raman spectroscopy. *Analyst*, *125*(2), 251–255. https://doi.org/10.1039/a908609i

Lees, A. C., & Pimm, S. L. (2015). Species, extinct before we know them? *Current Biology*, *25*(5), R177–R180. https://doi.org/10.1016/j.cub.2014.12.017

McConnaughey, T. A. (2003). Sub-equilibrium oxygen-18 and carbon-13 levels in biological carbonates: Carbonate and kinetic models. *Coral Reefs*, *22*(4), 316–327. https://doi.org/10.1007/s00338-003-0325-2

McConnaughey, T. A., Burdett, J., Whelan, J. F., & Paull, C. K. (1997). Carbon isotopes in biological carbonates: Respiration and photosynthesis. *Geochimica et Cosmochimica Acta*, *61*(3), 611–622. https://doi.org/10.1016/S0016-7037(96)00361-4

McConnaughey, T. A., & Gillikin, D. P. (2008). Carbon isotopes in mollusk shell carbonates. *Geo-Marine Letters*, *28*(5–6), 287–299. https://doi.org/10.1007/s00367-008-0116-4

Monismith, S. G., Genin, A., Reidenbach, M. A., Yahel, G., & Koseff, J. R. (2006). Thermally driven exchanges between a coral reef and the adjoining ocean. *Journal of Physical Oceanography*, *36*(7), 1332–1347. https://doi.org/10.1175/JPO2916.1

Monsecour, K. (2016). A new species of giant clam (Bivalvia: Cardiidae) from the Western Indian Ocean. *Conchylia*, *46*(1), 66–77.

Neo, M. L., Wabnitz, C. C., Braley, R. D., Heslinga, G. A., Fauvelot, C., Van Wynsberge, S., et al. (2017). Giant clams (Bivalvia: Cardiidae: Tridacninae): A comprehensive update of species and their distribution, current threats and conservation status. *Oceanography and Marine Biology: An Annual Review*, *55*, 87–387. https://doi.org/10.1201/b21944-5

Norton, J. H., & Jones, G. W. (1992). *The giant clam: An anatomical and histological atlas*, Canberra, Australia: Australian Centre for International Agricultural Research.

Owen, K., Charlton-Robb, K., & Thompson, R. (2011). Resolving the trophic relations of cryptic species: An example using stable isotope analysis of dolphin teeth. *PLoS ONE*, *6*(2), e16457. https://doi.org/10.1371/journal.pone.0016457

Pätzold, J., Heinrichs, J. P., Wolschendorf, K., & Wefer, G. (1991). Correlation of stable oxygen isotope temperature record with light attenuation profiles in reef-dwelling *Tridacna* shells. *Coral Reefs*, *10*(2), 65–69. https://doi.org/10.1007/BF00571825

Richter, C., Roa-Quiaoit, H., Jantzen, C., Al-Zibdah, M., & Kochzius, M. (2008). Collapse of a new living species of giant clam in the Red Sea. *Current Biology: CB*, *18*(17), 1349–1354. https://doi.org/10.1016/j.cub.2008.07.060

Roa-Quiaoit, H. A. F. (2005). The ecology and culture of giant clams (*Tridacnidae*) in the Jordanian sector of the Gulf of Aqaba. In *Red Sea*. *PhD*, Bremen, 12Germany: Universitat Bremen.

Romanek, C. S., Jones, D. S., Williams, D. F., Krantz, D. E., & Radtke, R. (1987). Stable isotopic investigation of physiological and environmental changes recorded in shell carbonate from the giant clam *Tridacna maxima*. *Marine Biology*, *94*(3), 385–393. https://doi.org/10.1007/BF00428244

Rosenfeld, M., Yam, R., Shemesh, A., & Loya, Y. (2003). Implication of water depth on stable isotope composition and skeletal density banding patterns in a *Porites lutea* colony: Results from a long-term translocation experiment. *Coral Reefs*, *22*(4), 337–345. https://doi.org/10.1007/s00338-003-0333-2

Schoepf, V., Stat, M., Falter, J. L., & McCulloch, M. T. (2015). Limits to the thermal tolerance of corals adapted to a highly fluctuating, naturally extreme temperature environment. *Scientific Reports*, *5*(1), 17,639. https://doi.org/10.1038/srep17639

Shaked, Y., Lazar, B., Marco, S., Stein, M., Tchernov, D., & Agnon, A. (2004). Evolution of fringing reefs: Space and time constraints from the Gulf of Aqaba. *Coral Reefs*, *24*(1), 165–172. https://doi.org/10.1007/s00338-004-0454-2

Su, Y., Hung, J.-H., Kubo, H., & Liu, L.-L. (2014). *Tridacna noae* (Röding, 1798)—A valid giant clam species separated from *T. maxima* (Röding, 1798) by morphological and genetic data. *The Raffles Bulletin of Zoology*, *62*, 124–135.

Swart, P. K., Leder, J. J., Szmant, A. M., & Dodge, R. E. (1996). The origin of variations in the isotopic record of scleractinian corals: II. Carbon. *Geochimica et Cosmochimica Acta*, *60*(15), 2871–2885. https://doi.org/10.1016/0016-7037(96)00119-6

Trofimova, T., Milano, S., Andersson, C., Bonitz, F. G. W., & Schöne, B. R. (2018). Oxygen isotope composition of *Arctica islandica* aragonite in the context of shell architectural organization: Implications for paleoclimate reconstructions. *Geochemistry, Geophysics, Geosystems*, *19*, 453–470. https://doi.org/10.1002/2017GC007239

Vermeij, G. J. (2013). The evolution of molluscan photosymbioses: A critical appraisal. *Biological Journal of the Linnean Society*, *109*(3), 497–511. https://doi.org/10.1111/bij.12095

Watanabe, T., Suzuki, A., Kawahata, H., Kan, H., & Ogawa, S. (2004). A 60-year isotopic record from a mid-Holocene fossil giant clam (*Tridacna gigas*) in the Ryukyu Islands: Physiological and paleoclimatic implications. *Palaeogeography, Palaeoclimatology, Palaeoecology*, *212*(3–4), 343354.

Weil, N. (2008, December). *Holocene coral reefs evolution in the Gulf of Eilat: Terraces, sea-levels and growth patterns (Masters)*. Jerusalem: Hebrew University of Jerusalem.

Welsh, K., Elliot, M., Tudhope, A., Ayling, B., & Chappell, J. (2011). Giant bivalves (*Tridacna gigas*) as recorders of ENSO variability. *Earth and Planetary Science Letters*, *307*(3-4), 266–270. https://doi.org/10.1016/j.epsl.2011.05.032

Yamanashi, J., Takayanagi, H., Isaji, A., Asami, R., & Iryu, Y. (2016). Carbon and oxygen isotope records from *Tridacna derasa* shells: Toward establishing a reliable proxy for sea surface environments. *PLoS ONE*, *11*(6), e0157659. https://doi.org/10.1371/journal.pone.0157659

Yau, A. J.-Y., & Fan, T.-Y. (2012). Size-dependent photosynthetic performance in the giant clam *Tridacna maxima*, a mixotrophic marine bivalve. *Marine Biology*, *159*(1), 65–75. https://doi.org/10.1007/s00227-011-1790-8

Yehudai, M., Lazar, B., Bar, N., Kiro, Y., Agnon, A., Shaked, Y., & Stein, M. (2017). U-Th dating of calcite corals from the Gulf of Aqaba. *Geochimica et Cosmochimica Acta*, *198*, 285–298. https://doi.org/10.1016/j.gca.2016.11.005

Yellowlees, D., Rees, T. A. V., & Leggat, W. (2008). Metabolic interactions between algal symbionts and invertebrate hosts. *Plant, Cell & Environment*, *31*(5), 679–694. https://doi.org/10.1111/j.1365-3040.2008.01802.x

Yonge, C. M. (1975). Giant clams. *Scientific American*, *232*(4), 96–105. https://doi.org/10.1038/scientificamerican0475-96

Young, S. G., & Bowman, A. W. (1995). Non-parametric analysis of covariance. *Biometrics*, *51*(3), 920–931.